A Discussion of Homoclinic Orbits in the Circular Restricted Three-Body Problem

Luke Bury & Don Kuettel

April 30, 2018

1 Introduction

LUKE SECTION

2 The Competition

LUKE SECTION

3 Circular Restricted Three Body Problem

Before studying periodic orbits, their manifolds, and the process of locating homoclinic orbits, it is necessary to provide the reader a solid foundation of the Circular Restricted Three Body Problem (CR3BP) - the dynamical system in which the aforementioned trajectories are created and analyzed. In the CR3BP (Fig. 1), the origin of the system is set at the barycenter of the two main bodies in the system (e.g., the Earth & Moon), and the frame rotates so these bodies remain stationary on the x-axis. The bodies are assumed to move in perfectly circular orbits and act as point masses from a gravitational perspective. The restricted problem is then to ascertain the motion of the third body whose mass is considered negligible. The system is typically normalized so that the masses of the two primary bodies sum to 1 (i.e., $m_1 = \mu$ and $m_2 = 1 - \mu$, where $\mu = m_2/(m_1 + m_2)$ is known as the three-body parameter), the distance between the primaries is 1, the orbital period period of the primaries is 2π, and the gravitational constant G is equal to 1. Under these conditions, the equations of motion for the CR3BP are shown in Equations 1-3:

$$\ddot{x} = 2\dot{y} + x - (1 - \mu)\left(\frac{x + \mu}{r_1^3}\right) - \mu\left(\frac{x - 1 + \mu}{r_2^3}\right) \tag{1}$$

$$\ddot{y} = -2\dot{x} + y\left(-\frac{1 - \mu}{r_1^3} - \frac{\mu}{r_2^3} + 1\right) \tag{2}$$

$$\ddot{z} = z\left(-\frac{1 - \mu}{r_1^3} - \frac{\mu}{r_2^3}\right), \tag{3}$$

where

$$r_1 = \sqrt{(x + \mu)^2 + y^2 + z^2} \tag{4}$$

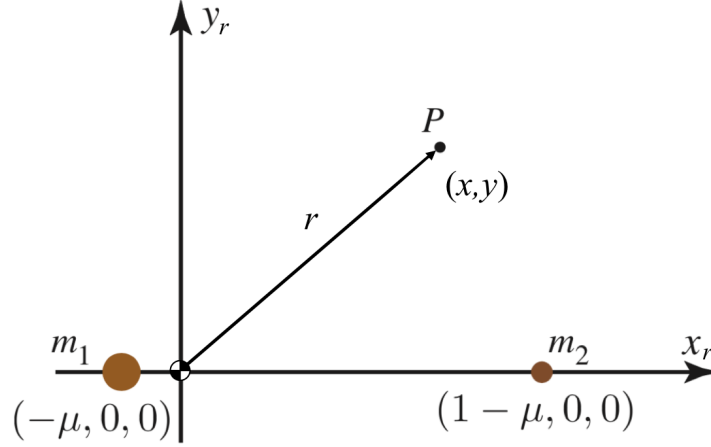$$r_2 = \sqrt{(x - 1 + \mu)^2 + y^2 + z^2}. \tag{5}$$

Figure 1: This figure shows the layout of the Circular Restricted Three-Body Problem [?]

In most simplified astrodynamic systems (e.g., Keplerian motion, CR3BP, n-body porblem, etc...), there are important parameters, known as integrals of motion, that are constant throughout the motion of a system that can be used to define the system. For example, the orbital elements of a trajectory in a Keplerian system are the system's integrals of motion. The integral of motion for the CR3PB is called the Jacobi constant and is given by

$$J = -\dot{x}^2 - \dot{y}^2 - \dot{z}^2 + x^2 + y^2 + \frac{2(1 - \mu)}{r_1} + \frac{2\mu}{r_2}. \tag{6}$$

For a given Jacobi constant, the motion of a particle is limited to certain regions of space due to the constraint that the velocity cannot have imaginary components. These restrictive regions, known as zero-velocity curves, are computed by setting the velocity in Equation 6 to zero and mapping the resultant surfaces in the CR3PB. The motion of an object with a specific Jacobi constant in bound within its respective zero-velocity curve and can only cross the boundaries under some non-conservative force.

3.1 Equilibrium Point Locations

Complex dynamical system such as the CR3PB often times have equilibrium points that result in a constant solution to the system's differential equations. In the CR3BP, these points, known as Lagrange points, mark positions where the combined gravitational pull of the two large masses provides precisely the centripetal force required to orbit with them (i.e., the Lagrange points are stationary within the rotating system of the CR3BP). There are five such points labeled L_1 - L_5 located in the plane of the two primary masses. The first three Lagrange points lie on the line connecting the two primary bodies, and the last two points, L_4 and L_5, are located at the vertex of an equilateral triangle formed with the two primary **bodies** [?].

2

In order to find the location of the five equilibrium points in the CR3BP, the velocity and acceleration must be set to zero in the system's equations of motion. This results in the following equations:

$$0 = x - (1 - \mu)\left(\frac{x + \mu}{r_1^3}\right) - \mu\left(\frac{x - 1 + \mu}{r_2^3}\right) \tag{7}$$

$$0 = y\left(-\frac{1 - \mu}{r_1^3} - \frac{\mu}{r_2^3} + 1\right) \tag{8}$$

$$0 = z. \tag{9}$$

If y is set to zero, a quintic equation in x emerges. Solving this equation to first order results in the following location for the first three Lagrange points:

$$L_1 = \left(1 - \left(\frac{\mu}{3}\right)^{1/3}, 0, 0\right) \tag{10}$$

$$L_2 = \left(1 + \left(\frac{\mu}{3}\right)^{1/3}, 0, 0\right) \tag{11}$$

$$L_3 = -\left(1 + \left(\frac{5\mu}{12}\right), 0, 0\right). \tag{12}$$

Using Equations 10-12 as initial conditions, a Newton-Raphson iteration can then be used to numerically find the exact location of the first three Lagrange points to machine precision. Equations 7-9 can also be used to find the two triangular equilibrium points, L$_4$ and L$_5$. Since the equilibrium points form an equilateral triangle with the primary bodies, $r_1 = r_2 = 1$ is substituted into Equation 7 and Equation 8. These equations are subsequently solved to provide the exact locations for the remaining equilibrium points:

$$L_4 = \left(\frac{1}{2} - \mu, \frac{\sqrt{3}}{2}, 0\right) \tag{13}$$

$$L_5 = \left(\frac{1}{2} - \mu, -\frac{\sqrt{3}}{2}, 0\right). \tag{14}$$

Using the Earth-Moon CR3BP three-body parameter ($\mu = 0.012155$), Table 1 shows the non-dimensional locations of the five Lagrange points to six significant digits. Additionally, Figure 2 graphically shows these locations along with a contour plot of the Earth-Moon CR3BP's zero-velocity curves for varying Jacobi constants. As Figure 2 shows, L$_1$, L$_2$, and L$_3$ lie at saddle points, while L$_4$ and L$_5$ lie at extrema values.

Table 1: Summary of the Dimensionless Earth-Moon CR3BP Equilibrium Points

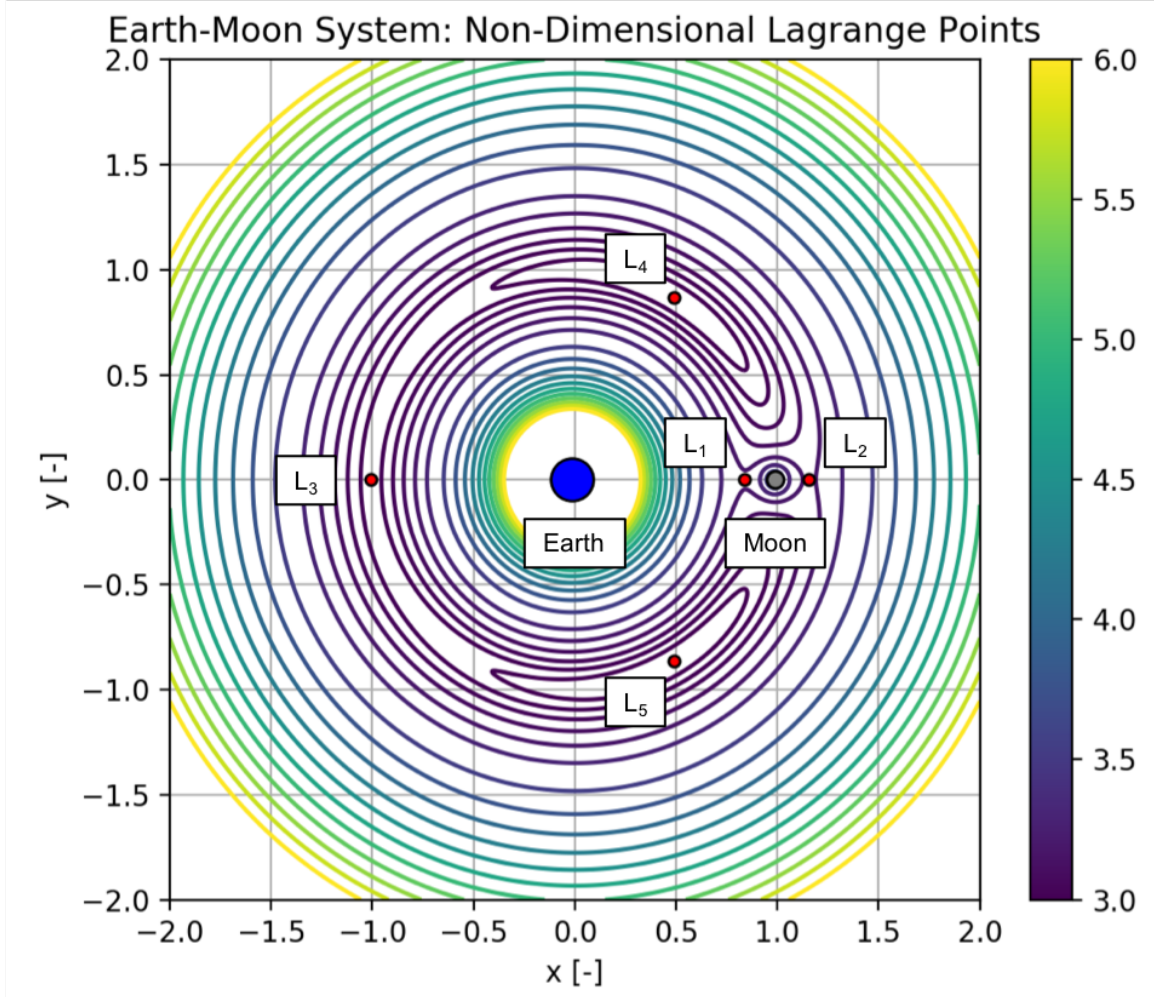| Lagrange Point	x	y	z
L_1	0.836893	0	0
L_2	1.15570	0	0
L_3	-1.00506	0	0
L_4	0.487845	0.866025	0
L_5	0.487845	-0.866025	0

Figure 2: This figure depicts the the 5 equilibrium points and the zero-velocity curves in the non-dimensional Earth-Moon CR3BP system.

3.2 Equilibrium Point Stability

In this section, a planar stability analysis is performed about each Lagrange point in the Earth-Moon CR3BP. This study entails linearizing the CR3BP equations of motion about each equilibrium solution and solving for the eigenvalues at the equilibrium point. The CR3BP equations of motion can be linearized by taking a Taylor series expansion of the ODE about each equilibrium point in

the system. Neglecting higher order terms, the linearized equations of motion are give by

$$\delta \begin{bmatrix} \dot{x} \\ \dot{y} \\ \ddot{x} \\ \ddot{y} \end{bmatrix} = Df\left(x^*, y^*, \dot{x}^*, \dot{y}^*\right) \begin{bmatrix} x \\ y \\ \dot{x} \\ \dot{y} \end{bmatrix}, \tag{15}$$

where

$$Df\left(x, y, \dot{x}, \dot{y}\right) = \begin{bmatrix} \frac{\partial \dot{x}}{\partial x} & \frac{\partial \dot{x}}{\partial y} & \frac{\partial \dot{x}}{\partial \dot{x}} & \frac{\partial \dot{x}}{\partial \dot{y}} \\ \frac{\partial \dot{y}}{\partial x} & \frac{\partial \dot{y}}{\partial y} & \frac{\partial \dot{y}}{\partial \dot{x}} & \frac{\partial \dot{y}}{\partial \dot{y}} \\ \frac{\partial \ddot{x}}{\partial x} & \frac{\partial \ddot{x}}{\partial y} & \frac{\partial \ddot{x}}{\partial \dot{x}} & \frac{\partial \ddot{x}}{\partial \dot{y}} \\ \frac{\partial \ddot{y}}{\partial x} & \frac{\partial \ddot{y}}{\partial y} & \frac{\partial \ddot{y}}{\partial \dot{x}} & \frac{\partial \ddot{y}}{\partial \dot{y}} \end{bmatrix}. \tag{16}$$

For the CR3BP, Equation 16 evaluates to

$$Df\left(x, y, \dot{x}, \dot{y}\right) = \begin{bmatrix} 0 & 0 & 1 & 0 \\ 0 & 0 & 0 & 1 \\ XX & XY & 0 & 2 \\ YX & YY & -2 & 0 \end{bmatrix}, \tag{17}$$

where

$$XX = \frac{\mu - 1}{r_1^3} - \frac{\mu}{r_2^3} + \frac{3\mu\left(\mu + x - 1\right)^2}{r_2^5} - \frac{3\left(\mu + x\right)^2\left(\mu - 1\right)}{r_1^5} + 1 \tag{18}$$

$$XY = YX = \frac{3\mu y\left(\mu + x - 1\right)}{r_2^5} - \frac{3y\left(\mu + x\right)\left(\mu - 1\right)}{r_1^5} \tag{19}$$

$$YY = \frac{\mu - 1}{r_1^3} - \frac{\mu}{r_2^3} + \frac{3\mu y^2}{r_2^5} - \frac{3y^2\left(\mu - 1\right)}{r_1^5} + 1. \tag{20}$$

By evaluating the matrix given in Equation 17 at the equilibrium points and finding the resulting eigenvalues of the matrix, the stability of that point can be ascertained.

3.2.1 L_1, L_2, and L_3 Stability

It was visually shown in Figure 2 that L_1, L_2, and L_3 were saddle points. By plugging in the locations of the equilibrium points given in Table 1 along with the Earth-Moon three-body parameter ($\mu = 0.012155$), this claim can be mathematically validated.

L$_1$

The evaluated Df matrix for the L$_1$ Lagrange point is given by

$$Df|_{L_1} = \begin{bmatrix} 0 & 0 & 1 & 0 \\ 0 & 0 & 0 & 1 \\ 11.2955 & 0 & 0 & 2 \\ 0 & -4.1478 & -2 & 0 \end{bmatrix}, \tag{21}$$

where

$$\lambda_{1,2} = \pm 2.9321 \text{ and } \lambda_{3,4} = \pm i2.3344. \tag{22}$$

As Equation 22 shows, the L$_1$ equilibrium point has a positive, real eigenvalue that results in a dynamically unstable saddle point. Small departures from the equilibrium will grow exponentially with a time constant of $\tau = 1/real(\lambda_{3,4}) = 0.4284$. Re-dimensionalizing this value by the rotation rate of the Earth-Moon system ($\omega = 2.665 \times 10^{-6}$ rad/sec) results in a time constant of $\tau \approx 1.86$ days. In other words, a satellite parked at L$_1$ will wander off after a few days unless course corrections are made.

L$_2$

The evaluated Df matrix for the L$_2$ Lagrange point is given by

$$Df|_{L_2} = \begin{bmatrix} 0 & 0 & 1 & 0 \\ 0 & 0 & 0 & 1 \\ 7.3807 & 0 & 0 & 2 \\ 0 & -2.1903 & -2 & 0 \end{bmatrix}, \tag{23}$$

where

$$\lambda_{1,2} = \pm 2.1586 \text{ and } \lambda_{3,4} = \pm i1.8626. \tag{24}$$

Similarly to the L$_1$ point, the L$_2$ Lagrange point has a positive, real eigenvalue that results in a dynamically unstable saddle point. The re-dimensionalized L$_2$ time constant is $\tau \approx 2.33$ days.

L$_3$

The evaluated Df matrix for the L$_3$ Lagrange point is given by

$$Df|_{L_3} = \begin{bmatrix} 0 & 0 & 1 & 0 \\ 0 & 0 & 0 & 1 \\ 3.0214 & 0 & 0 & 2 \\ 0 & -0.0107 & -2 & 0 \end{bmatrix}, \tag{25}$$

where

$$\lambda_{1,2} = \pm 0.1779 \text{ and } \lambda_{3,4} = \pm i1.0104. \tag{26}$$

Once again, the evaluated Df matrix has a positive, real eigenvalue resulting in the L_3 Lagrange point being unstable. The re-dimensionalized L_3 time constant is $\tau \approx 4.30$ days.

3.2.2 L_4 and L_5 Stability

The stability analysis of the L_4 and L_5 Lagrange points yields a surprise. While these points correspond to local maxima of the total potential, they are stable due to a "Coriolis" force. Initially, a mass situated near L_4 or L_5 will tend to slide down the potential, but as it does, it picks up speed sending it into an orbit around the equilibrium point. To prove this, the evaluated Df matrix for the L_4 and L_5 Lagrange points is given by

$$Df|_{L_{4,5}} = \begin{bmatrix} 0 & 0 & 1 & 0 \\ 0 & 0 & 0 & 1 \\ 0.7500 & \pm 1.2675 & 0 & 2 \\ \pm 1.2675 & 2.2500 & -2 & 0 \end{bmatrix}, \tag{27}$$

where

$$\lambda_{1,2} = \pm i0.9545 \text{ and } \lambda_{3,4} = \pm i0.2983. \tag{28}$$

As Equation 28 shows, the L_4 and L_5 equilibrium points have purely imaginary eigenvalues in the Earth-Moon system resulting in Lyapunov stability. However, this is not always the case for a three body system. In order for the L_4 and L_5 Lagrange points to be stable, the primary masses of the system have to satisfy the follow **inequality** [?]

$$\frac{m_1}{m_2} > \frac{25 + \sqrt{621}}{2} \approx 24.96. \tag{29}$$

For reference, $m_1/m_2 = 81.27$ for the Earth-Moon system. Now that the Earth-Moon equilibrium points have been identified, numerical methods can be used to generate families of periodic orbits about the points.

3.3 Periodic Orbits

The solution flow of a dynamical system is often times denoted $x(t) = \varphi(t; x_0)$ with initial condition $x(t_0) = \varphi(t_0; x_0)$. A periodic orbit is a solution of the system such that $\varphi(t + T; x_0) = \varphi(t; x_0)$ for all t where $T > 0$ is the period of the orbit. Lyapunov's Center Theorem then states that for a system with an integral of motion (the Jacobi constant in the case of the CR3BP), if $Df(x^*)$ has eigenvalues $\pm i\omega, \lambda_3, \lambda_4, ..., \lambda_n$, then there exists a one-parameter family of periodic orbits emanating from the equilibrium point. Furthermore, periods tend to $2\pi/\omega$ when approaching the equilibrium point along the **family** [?]. Using this knowledge, one of the most straightforward methods used to solve for periodic orbit families is to make educated guesses at individual periodic orbit initial conditions and then use a single shooter algorithm to correct them.

3.3.1 Family Finding Algorithm

The family finding algorithm (FFA) begins by determining the dynamical system's fundamental matrix $\Phi(t, t_0)$. In a system as complicated as the CR3BP, Φ must be computed numerically through the following differential equation

$$\dot{\Phi} = Df(x)\Phi \text{ with } \Phi(t_0, t_0) = \mathcal{I}. \tag{30}$$

The full dynamics matrix Df, which was touched on in Equation 17, is given by

$$Df = \begin{bmatrix} 0_{3\times3} & \mathcal{I}_{3\times3} \\ \Omega_{i,j} & V \end{bmatrix} \tag{31}$$

where, 0 is a 3×3 zero matrix, $\mathcal{I}$ is a 3×3 identity matrix, V is given by

$$V = \begin{bmatrix} 0 & 2 & 0 \\ -2 & 0 & 0 \\ 0 & 0 & 0 \end{bmatrix}, \tag{32}$$

and $\Omega_{i,j}$ is a 3×3 matrix of second order partial derivatives $(\Omega_{i,j} = \Omega_{j,i})$ given by

$$\Omega_{x,x} = \frac{\partial \ddot{x}}{\partial x} = \frac{\mu - 1}{r_1^3} - \frac{\mu}{r_2^3} + \frac{3\mu(\mu + x - 1)^2}{r_2^5} - \frac{3(\mu + x)^2(\mu - 1)}{r_1^5} + 1 \tag{33}$$

$$\Omega_{y,y} = \frac{\partial \ddot{y}}{\partial y} = \frac{\mu - 1}{r_1^3} - \frac{\mu}{r_2^3} + \frac{3\mu y^2}{r_2^5} - \frac{3y^2(\mu - 1)}{r_1^5} + 1 \tag{34}$$

$$\Omega_{z,z} = \frac{\partial \ddot{z}}{\partial z} = \frac{\mu - 1}{r_1^3} - \frac{\mu}{r_2^3} + \frac{3\mu z^2}{r_2^5} - \frac{3z^2(\mu - 1)}{r_1^5} \tag{35}$$

$$\Omega_{x,y} = \frac{\partial \ddot{x}}{\partial y} = \frac{3\mu y(\mu + x - 1)}{r_2^5} - \frac{3y(\mu + x)(\mu - 1)}{r_1^5} \tag{36}$$

$$\Omega_{y,z} = \frac{\partial \ddot{y}}{\partial z} = \frac{3\mu z(\mu + x - 1)}{r_2^5} - \frac{3z(\mu + x)(\mu - 1)}{r_1^5} \tag{37}$$

$$\Omega_{z,x} = \frac{\partial \ddot{z}}{\partial x} = \frac{3\mu yz}{r_2^5} - \frac{3yz(\mu - 1)}{r_1^5}. \tag{38}$$

8

Using the aforementioned Lyapunov Center Theorem, the FFA is initiated by perturbing the equilibrium point of interest in the direction of a center manifold (purely imaginary eigenvalue) by a small amount ($\epsilon < 1 \times 10^{-4}$). This results in the "smallest" periodic orbit around the equilibrium point. The period of the orbit is then determined by the value of the eigenvalue ($T = 2\pi/\lambda$). To continue the FFA, future periodic orbit initial conditions ($\boldsymbol{x}_0, T$) are calculated by adding small perturbations to the previous periodic orbit initial conditions ($\tilde{\boldsymbol{x}}_0, \tilde{T}$) in the orbit tangent direction ($\tilde{\boldsymbol{x}}_0', \tilde{T}'$). This update is mathematically shown as follow

$$\boldsymbol{x}_0 = \tilde{\boldsymbol{x}}_0 + \Delta s \tilde{\boldsymbol{x}}_0' \tag{39}$$

$$T = \tilde{T} + \Delta s \tilde{T}', \tag{40}$$

where Δs is the step size between the original periodic orbit and the new periodic orbit and ($\tilde{\boldsymbol{x}}_0', \tilde{T}'$) is the change in ($\boldsymbol{x}_0, T$) between two previous orbits. In order to insure that the new periodic orbit is part of the periodic orbit family, two important constraints must be satisfied. The first constraint, known as the Poincaré phase condition, which assumes that a periodic orbit in the family has already been computed, states that

$$< \boldsymbol{x}_0 - \tilde{\boldsymbol{x}}_0, \boldsymbol{f}\left(\tilde{\boldsymbol{x}}_0\right) >= 0, \tag{41}$$

where $\boldsymbol{f}\left(\boldsymbol{x}\right)$ are the dynamics of the CR3BP evaluated at some state. The second constraint, known as the pseudo-arclength continuation constraint, which assumes that a periodic orbit in the family and an approximation of the tangent to the solution family has already been computed, states that

$$< \boldsymbol{x}_0 - \tilde{\boldsymbol{x}}_0, \tilde{\boldsymbol{x}}_0' > + \left(T - \tilde{T}\right)\tilde{T}' = \Delta s. \tag{42}$$

Using these constraints, a system of equations for the FFA is given by

$$\begin{bmatrix} \boldsymbol{\varphi}\left(T; \boldsymbol{x}_0\right) - \boldsymbol{x}_0 \\ < \boldsymbol{x}_0 - \tilde{\boldsymbol{x}}_0, \boldsymbol{f}\left(\tilde{\boldsymbol{x}}_0\right) > \\ < \boldsymbol{x}_0 - \tilde{\boldsymbol{x}}_0, \tilde{\boldsymbol{x}}_0' > + \left(T - \tilde{T}\right)\tilde{T}' - \Delta s \end{bmatrix} = \boldsymbol{F}\left(\boldsymbol{x}_0, T\right) = \boldsymbol{0}, \tag{43}$$

where $\boldsymbol{x}_0$ and T are unknowns. This system of equations is then solved using a single shooter **algorithm [?]** which is given in the form

$$\begin{bmatrix} \Phi\left(T\right) - \mathcal{I}_{n \times n} & \boldsymbol{f}\left(\boldsymbol{x}\left(T\right)\right) \\ \dot{\tilde{\boldsymbol{x}}}_0 & 0 \\ \tilde{\boldsymbol{x}}_0' & \tilde{T}' \end{bmatrix} \begin{bmatrix} \delta \boldsymbol{x}_0 \\ \delta T \end{bmatrix} = -\boldsymbol{F}\left(\boldsymbol{x}_0, T\right), \tag{44}$$

where $\delta \boldsymbol{x}_0$ and δT are updates to the initial conditions of the new periodic orbit. Since the single shooter algorithm uses a first-order Newton-Raphson method, Equation 44 is iterated until convergence. Furthermore, since this system is overdetermined ($n+2$ equations and $n+1$ unknowns), a pseudo-inverse is used when solving for $\delta \boldsymbol{x}_0$ and δT. An example of the single shooter algorithm

correcting a periodic orbit is shown in Figure 3. Using this FFA, a periodic orbit family can be calculated with minimal a priori knowledge for as many number of periodic orbits as desired.
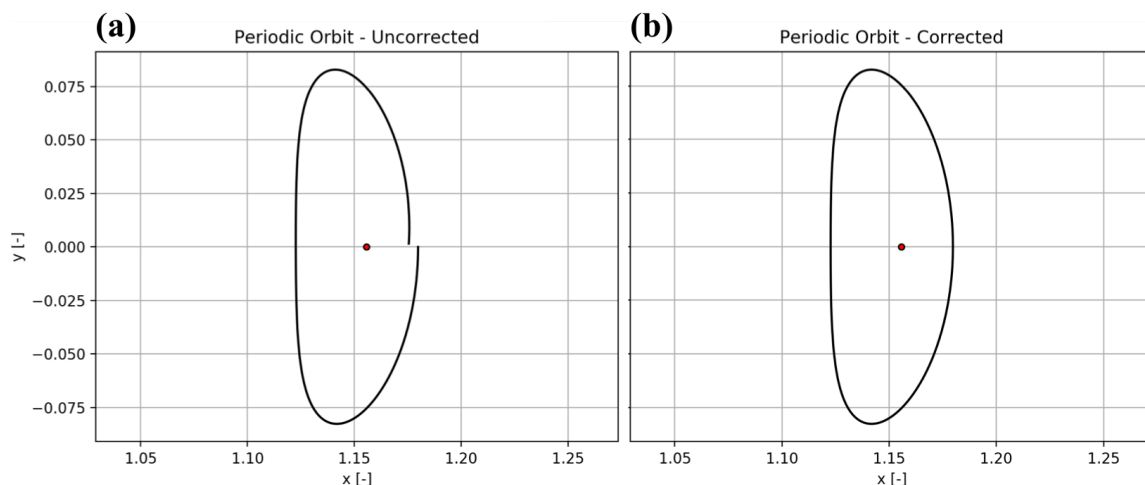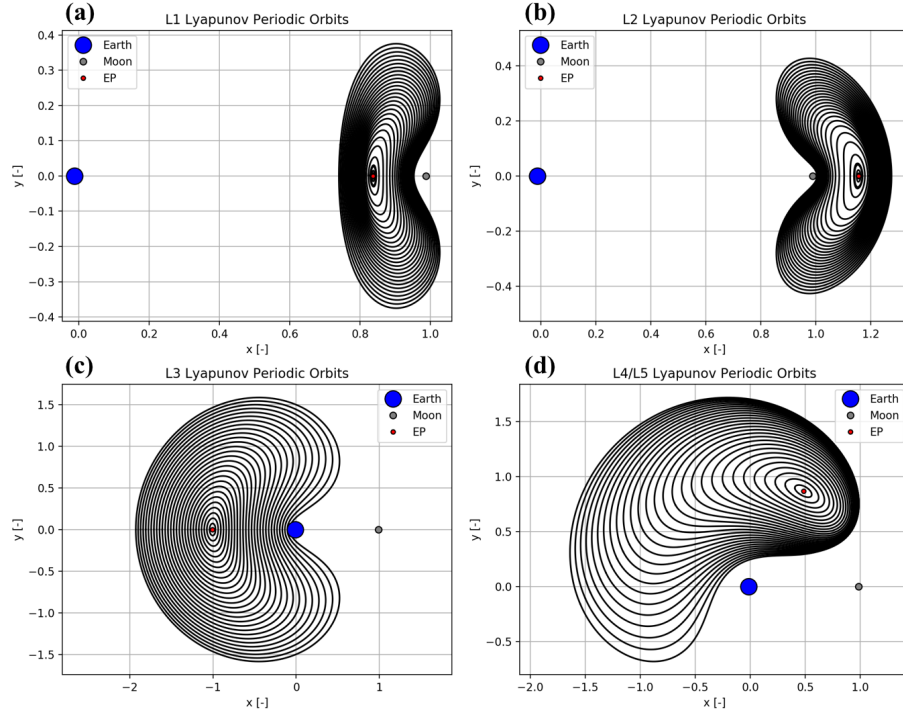

Figure 3: This figure shows the single shooter algorithm correcting a periodic orbit. Figure (a) shows the uncorrected orbit, and Figure (b) shows the correct orbit.

3.3.2   Orbit Families

In 1892, Poincaré showed that an infinite number of periodic solutions exist in the three-body problem. These solutions come in a variety of forms that include planar Lypaunov periodic orbits, 3-dimensional clamshell orbits, 3-dimensional halo orbits, and many others.

Figure 4: This figure shows the single shooter algorithm correcting a periodic orbit. Figure (a) shows the uncorrected orbit, and Figure (b) shows the correct orbit.
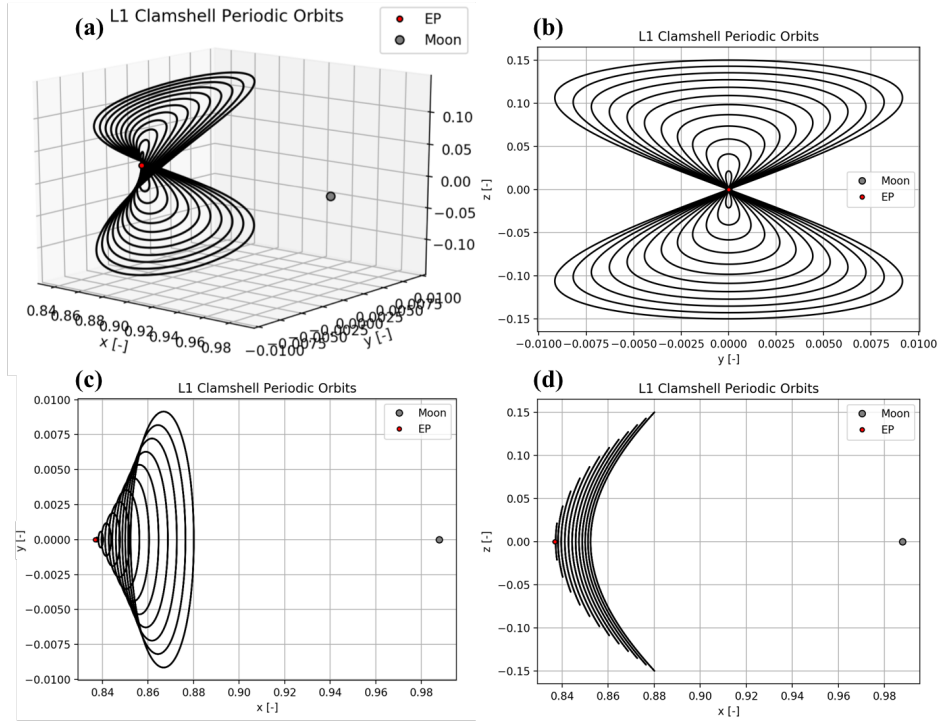

Figure 5: This figure shows the single shooter algorithm correcting a periodic orbit. Figure (a) shows the uncorrected orbit, and Figure (b) shows the correct orbit.

4   Conclusion

LUKE SECTION